

## Percolation Threshold for Electronic Conduction in $\beta$ -Alumina-Type Compounds

M. SANKARARAMAN, RYOICHI KIKUCHI,<sup>1</sup> AND HIROSHI SATO

*School of Materials Engineering, Purdue University, West Lafayette, Indiana 47907*

Received March 7, 1990

DEDICATED TO J. M. HONIG ON THE OCCASION OF HIS 65TH BIRTHDAY

It is found that the addition of more than a certain amount of mixed valent ions would be necessary to render mixed conducting characteristics to  $\beta$ -alumina-type compounds. Based on the assumption that the electronic conduction is due to the hopping of small polarons to the nearest neighboring ions on the octahedral sites in the spinel block of  $\beta$ -alumina similar to that in magnetite, the pair approximation of the cluster variation method indicates that the threshold composition of such a mixed valent additive must exceed at least 0.24 of the number of octahedral ions. A new method of calculating the percolation limit is shown. © 1990 Academic Press, Inc.

### 1. Introduction

$\beta$ -alumina is known to have an unusually high ionic conductivity due to its peculiar structure. On the other hand, its electronic conductivity is known to be very small. Because of these properties,  $\beta$ -alumina-type compounds have been considered to be good candidates for solid electrolytes for various applications. However, if the electronic conductivity can be enhanced appreciably, these materials can be used as good electrode materials, especially when  $\beta$ -alumina is used as a solid electrolyte due to the compatibility. Hence, the possibility of doping  $\beta$ -alumina with different metal ions which may lead to electronic conductivity has been examined.

<sup>1</sup> Permanent address: Department of Materials Science and Engineering, University of California—Los Angeles, Los Angeles, CA 90024.

It has been customarily considered that an addition of mixed valent ions to  $\beta$ -alumina would enhance the electronic conductivity due to the release of electrons, thus leading to mixed conductivity. Rather extensive trials have been made in this direction, but none has been too successful. Examinations of the mechanism of electronic conduction in  $\beta$ -alumina-type compounds, however, have led to a conclusion that the addition of mixed valent ions beyond a certain amount (percolation threshold) may be necessary.

The purpose of this note is to examine briefly the required conditions for such addition of mixed valent ions to enhance electronic conductivity. We will also give a new type of calculation by means of the pair approximation of the cluster variation method (CVM; *1*) which can predict the percolation limit for the electronic conduction in a system that is characteristic to  $\beta$ -alumina-type structure.

## 2. Electronic Conductivity in $\beta$ -Alumina

It is generally believed that an addition of a small amount of mixed valent ions to  $\beta$ -alumina-type compounds would be enough to create electronic conduction in these compounds as this would release electrons to the system. However, past efforts of this kind failed to show any appreciable electronic conductivity in  $\beta$ -alumina. For example, Galli *et al.* (2) reported the electronic transport number to be essentially zero for undoped, 0.5 wt% MgO-doped, 3.8 wt% Fe<sub>2</sub>O<sub>3</sub>-doped, and 3.57 wt% CoO plus 1.28 wt% TiO<sub>2</sub>-doped  $\beta$ -aluminas. More recently, Kennedy *et al.* (3–8) and Vest *et al.* (9–12) doped a rather large amount of Fe ions to replace Al ions to achieve this goal, but could not enhance the electronic conductivity appreciably. These results indicate that the problem requires further attention.

The structure of  $\beta$ -alumina has been investigated in detail (12, 13). However, for the present purpose, it is easier to view the structure as a modulated structure of spinel by loose conduction layers at every fifth close-packed oxygen layer in the direction perpendicular to them (the *c*-direction) (14, 15). In other words, between the two conduction layers, the structure is identical to that of spinel except for the arrangements of metallic ions immediately neighboring the conduction layer.

A well-known electronic conductor with the spinel structure is magnetite, Fe<sub>3</sub>O<sub>4</sub>. Magnetite has the inverse spinel structure, in which the tetrahedral sites are occupied by trivalent Fe<sup>3+</sup> ions while the octahedral sites are occupied by Fe<sup>2+</sup> and Fe<sup>3+</sup> ions randomly. The hopping of electrons between Fe<sup>2+</sup> and Fe<sup>3+</sup> ions (or more precisely in the form of small polarons) among the nearest neighboring octahedral sites is considered to be the origin of the electronic conduction (16, 17). If this is the case for  $\beta$ -alumina, then mixed valent ions of the same type should exist on the octahedral sites in

different valences and the amount of these mixed valent ions should be enough to form a percolation path for electrons (polarons).

Unlike the spinel MgAl<sub>2</sub>O<sub>4</sub>, in the spinel block of  $\beta$ -alumina trivalent Al ion occupies both the tetrahedral and the octahedral sites, although the tetrahedral sites preferentially accept divalent spinel-forming ions such as Mg<sup>2+</sup>, Zn<sup>2+</sup>, or transition metal ions such as Ni<sup>2+</sup> and Co<sup>2+</sup>. Hence, the spinel block in  $\beta$ -alumina is not neutral but has excess charge in the idealized Beever-Ross structure (14). In other words, the valence state of metallic ions in the spinel block of  $\beta$ -alumina should, on the average, be trivalent. Therefore, unless the charge compensation condition changes, Fe ions which can take both divalent and trivalent state would be in the trivalent state, even if they go into the octahedral sites, and, hence, would not be effective enough to create appreciable electronic conductivity. Results of Kennedy *et al.* (3–8) and Vest *et al.* (9–11) seem to be consistent with this statement.

A different possibility exists in the case of the addition of Ti ions which prefers the octahedral sites, in the spinel structure. Ti ions can take Ti<sup>2+</sup>, Ti<sup>3+</sup>, and Ti<sup>4+</sup> states depending on the condition, but if doped alone, Ti might go in the trivalent state replacing Al<sup>3+</sup> in octahedral sites for the reasons mentioned above. However, divalent ions such as Ni<sup>2+</sup> and Co<sup>2+</sup> enter preferentially into the tetrahedral sites which has been proved by optical absorption spectrum (18) and X-ray structural analysis (19). Therefore, if Ti ions are doped along with Ni<sup>2+</sup> ions, Ni<sup>2+</sup> ions occupying the tetrahedral sites might force the Ti ions on the octahedral sites to exist as Ti<sup>3+</sup> and Ti<sup>4+</sup>. If this is the case, enough amount of mixed valent ions on the octahedral sites such as Ti would create the electronic conduction.

It is interesting to know, at least approximately, the amount of mixed valent ions to be added to the octahedral sites of  $\beta$ -alumina to create the electronic conductivity. In or-

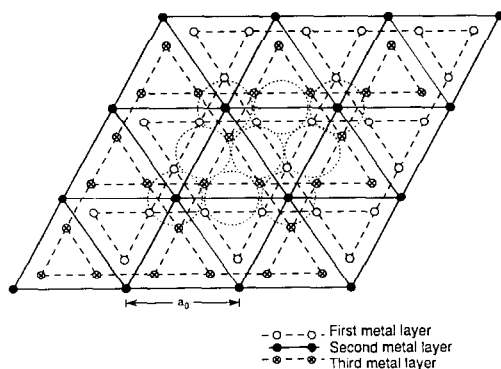


FIG. 1. Projection of the network of the octahedral sites in the spinel block of the  $\beta$ -alumina-type structure along the  $c$ -axis.  $\circ$  and  $\otimes$ , Kagomé lattice;  $\bullet$ , triangular lattice.

der to know this, it is necessary to know the structure of the conduction path or the distribution of connected octahedral sites in  $\beta$ -alumina. As explained earlier,  $\beta$ -alumina is a modulated structure of spinel at every fifth close-packed layer of oxygen in the  $c$ -direction by a loose conduction layer across which the octahedral sites are separated. In other words, the conduction path of  $\beta$ -alumina is a two-dimensional network. If we plot the network of such octahedral sites, these form three layers of two-dimensional network as shown in Fig. 1. The upper and the lower layers are the two-dimensional Kagomé lattices, (20), which are connected by a triangular lattice in the middle. Other metallic sites exist above and below the two Kagomé layers, but can be neglected as they do not contribute to the percolation. In the triangular lattice in the middle layer alone, because the distance between sites of the triangular lattice is larger than the nearest neighboring sites, no percolation path exists in this plane. In this respect, the percolation limit in such a percolation path in  $\beta$ -alumina should be practically determined by that of the two dimensional Kagomé lattice, but modified somewhat by the existence of the middle layer.

The determination of the percolation limit

was treated earlier by the cluster variation method as the lowest concentration limit of magnetic atoms for the appearance of the spontaneous magnetization in magnetically dilute systems (21). The problem was also treated as a dynamical bond percolation problem such as the tracer diffusion in binary mixture lattice gas by means of the path probability method (PPM) of irreversible statistical mechanics (22). Both the methods give identical values for the percolation limit (22). For a regular lattice, the pair approximation of the CVM gives the value for the percolation limit  $\rho_c$  to be equal to  $1/(2\omega - 1)$ , where  $2\omega$  is the coordination number of the lattice. In the case of the two-dimensional Kagomé lattice,  $2\omega = 4$  and, hence,  $\rho_c$  is equal to  $1/3$ . If the triangle approximation of the CVM is used,  $\rho_c$  is found to be  $1/2$ . A higher degree of approximation gives a higher value of  $\rho_c$  and it is expected that the exact value would not be smaller than  $1/2$ .

The existence of the middle triangular layer would modify the value of the percolation limit. Because each triangular lattice site has three nearest neighboring sites on both the upper and the lower Kagomé lattices (Fig. 1), the coordination number is six. Therefore, the percolation limit is not readily given by the formula  $1/(2\omega - 1)$ . As it is of interest to know the effect of the middle layer on the percolation limit, a new type of calculation by means of the CVM was carried out and the treatment is given in detail in Appendix. The pair approximation gives the value of 0.24 instead of  $1/3$ , indicating the effect of the middle layer is considerable. The calculation in terms of the triangular approximation is now in progress. The value of the percolation limit in triangle approximation or of the higher approximation is expected to be substantially higher than the value of 0.24.

### 3. Conclusions

Factors which would make  $\beta$ -alumina-type compounds mixed conducting are ex-

amined. It would most probably require the addition of mixed valent ions with valences 3+ and 4+ such as Ti on the octahedral sites. Codoping of divalent ions such as Co and Ni which would occupy the tetrahedral sites and which would allow ions on the octahedral sites to take valences higher than three is most probably required. The amount of such mixed valent ions which occupy the octahedral sites should be 24% or more if it is at all possible. Factors pointed out above constitute the difficulty of producing mixed conducting  $\beta$ -alumina-type compounds.

Since the conduction path of  $\beta$ -alumina is composed of two layers of two-dimensional Kagomé lattices and a two-dimensional triangular lattice in the middle, a new type of calculation of the percolation limit  $\rho_c$ , in the form of phase transition for the percolation, (23), by means of the pair approximation of the CVM is presented in the Appendix. In the pair approximation, the existence of the middle layer is found to lower the percolation limit of the Kagomé lattice, from 1/3 to 0.24. Such a large effect is somewhat surprising, and the calculation by a higher degree of approximation is being made to examine the effect.

## Appendix

### Theory of Percolation Limit

#### A1. Introduction

This appendix presents details of how the percolation is calculated for two lattice structures. The first is the two-dimensional Kagomé lattice and the second consists of two parallel Kagomé planes connected by a middle layer of the triangular lattice shown in Fig. 1. The middle layer is drawn with black dots and the upper and lower Kagomé lattices with open circles.

The calculation uses the pair approximation of the cluster variation method (CVM; 1). We use the basic principle of the

percolation treatment proposed before (23), and it is summarized in Section A2. After the brief discussion of the Kagomé lattice in Section A3, we present the three-layer case in detail in Section A4.

#### A2. Percolation Treated as a Phase Transition

In a system of  $N$  lattice points, we distribute  $\rho N$  particles, leaving  $(1 - \rho)N$  points vacant. When two particles are on nearest-neighbor lattice points, we define that they are connected and are in a connected cluster. In the equilibrium state, when  $\rho$  is small, all connected clusters are of finite sizes. When  $\rho$  exceeds a critical value  $\rho_c$ , there can be an infinitely extended cluster and we call the state percolating. This model is called the "site" percolation problem, in contrast to the "bond" problem in which open and blocked nearest-neighbor bonds are distributed over the lattice (24).

We assign a sign, + or -, to each particle, with the condition that all particles in a connected cluster have the same sign. Then a particle pair has a form (+ +) or (- -), but not (+ -). If the sign of a cluster is assigned randomly, then,

(i) in the nonpercolating state, each + cluster of a certain size can have a matching cluster, in a system of infinitely large  $N$  and

(ii) in the percolating state, we can prove (23) that there can be only one infinitely extended cluster, which takes either a + or -. Since there is no matching cluster to an infinitely extended cluster, the total number of + particles and that of - particles become unequal. This is equivalent to the magnetized state in the Ising model ferromagnetism.

Based on the properties (i) and (ii), we can formulate the percolation properties in analogy with the second-order phase transition in the Ising model ferromagnetism. The nonpercolating state corresponds to the disordered paramagnetic state, while the state of the critical density  $\rho_c$  corresponds to the

density at which the long range order vanishes or to the ferromagnetic Curie point (23).

We can take into account the case in which particles are interacting, as was done in Ref. (23) but, in the present work, we assume no such interactions among particles.

### A3. Kagomé Lattice Percolation

We treat the Kagomé lattice percolation using the pair approximation of the CVM.

A lattice point is either empty or occupied by a + or a - particle. The probabilities of the three are written as  $x_i$  with  $i = 0, 1, \text{ or } 2$ , respectively. The configuration of a pair of nearest neighbor points is one of  $(i, j)$  with the condition that  $(1, 2)$  and  $(2, 1)$  are excluded. The probability of  $(i, j)$  is written as  $y_{ij}$ .

If the number of triangles in the Kagomé lattice is written as  $2M$ , then the number of lattice points is  $3M$  and the number of nearest-neighbor pairs is  $6M$ . The coordination number is  $2\omega = 4$ . The entropy expression is written in the pair approximation of the CVM as

$$S_{3M} = 3MK \left[ \sum_{i=0}^2 L(x_i) - 2 \sum_{i,j}^* L(y_{ij}) + 1 \right], \quad (1)$$

where  $\sum_{i,j}^*$  indicates the sum over  $i$  and  $j$  except  $(1, 2)$  and  $(2, 1)$ , and  $L(x)$  is defined as

$$L(x) \equiv x \ln x - x. \quad (2)$$

When the particles are not interacting, the particle distribution is homogeneous with the probability  $\rho$  at every point. The particle-particle pair probability is  $\rho^2$ .

In the percolating state in which the densities of + and - particles are different,  $x_1$  and  $x_2$  are different. We introduce the long-range order variable  $\xi_1$  as

$$2\xi_1 \equiv x_1 - x_2. \quad (3a)$$

Similarly for a particle pair we define

$$2\xi_2 \equiv y_{11} - y_{22}. \quad (3b)$$

Using these long-range orders, the  $x$  and  $y$  variables are written as

$$x_i = \frac{1}{2}\rho - (-1)^i \xi_1$$

$$y_{ii} = \frac{1}{2}\rho^2 - (-1)^i \xi_2 \quad (i = 1 \text{ or } 2) \quad (4)$$

$$y_{oi} = \frac{1}{2}\rho(1 - \rho) - (-1)^i(\xi_1 - \xi_2).$$

The  $\rho_c$  point can be determined by the vanishing of the Hessian determinant. The latter is obtained by the second derivatives of the entropy with respect to the two long-range variables,  $\xi_1$  and  $\xi_2$ . Algebraic transformations lead to

$$\rho_c = \frac{1}{3}, \quad (5a)$$

which is the  $\omega = 2$  case of the general expression of the pair approximation (21, 23):

$$\rho_c = \frac{1}{2\omega - 1}. \quad (5b)$$

### A4. Percolation in the Three-Layer Structure

The three layer structure is illustrated in Fig. 1. The middle layer points, marked black, connect triangles in the two Kagomé layers.

As the occupation variables we use  $x_i$ 's and  $y_{ij}$ 's, for the two Kagomé planes as defined in Section A3. The occupation variables for the middle layer are written as  $v_i$ . The definition of  $i = 0, 1, \text{ and } 2$  is the same as  $i$  for  $x_i$ 's in Section A3. For the bond connecting a Kagomé layer point and the middle layer point, we write the occupation probability as  $z_{ij}$ , where the first subscript is for the Kagomé layer and the second one is for the middle layer point. As was done in

Section A3,  $(i, j) = (1, 2)$  and  $(2, 1)$  are excluded.

Corresponding to Eqs. (3a) and (3b), we introduce two more long-range order variables  $\xi_3$  and  $\xi_4$  by

$$\begin{aligned} 2\xi_3 &\equiv v_1 - v_2, \\ 2\xi_4 &\equiv z_{11} - z_{22}. \end{aligned} \tag{6}$$

The relations in Eq. (4) hold unchanged for  $x_i$ 's and  $y_{ij}$ 's for the Kagomé planes. The  $v_i$  and  $z_{ij}$  variables are written as linear combinations of  $\xi_1, \xi_3,$  and  $\xi_4$  as

$$\begin{aligned} v_i &= \frac{1}{2}\alpha\rho - (-1)^i\xi_3 \\ z_{ii} &= \frac{1}{2}\alpha\rho^2 - (-1)^i\xi_4 \quad i = 1 \text{ or } 2 \\ z_{i0} &= \frac{1}{2}\rho(1 - \alpha\rho) - (-1)^i(\xi_1 - \xi_4) \\ z_{oi} &= \frac{1}{2}\alpha\rho(1 - \rho) - (-1)^i(\xi_3 - \xi_4). \end{aligned} \tag{7}$$

In writing these variables we have introduced a parameter  $\alpha$  to indicate the ratio of particles allowed to come on a middle layer point and those on the Kagomé layer point. When  $\alpha = 0$ , no particles are allowed to come to the middle layer point, while  $\alpha = 1$  corresponds to the case where the occupation probability is the same on every point in the system.

We write the number of the middle layer

point as  $M$ . This  $M$  has the same meaning as  $M$  in Section A2. The total number of points on the two Kagomé layers is  $6M$  and the total number of nearest-neighbor pairs in the two Kagomé layers is  $12M$ . The number of pairs connecting the two Kagomé layer points and the middle layer points is  $6M$ .

Making use of these numbers, the entropy expression of the pair approximation can be written using, for example, Barker's procedure (24) as

$$\begin{aligned} S_M &= kM \left[ 24 \sum_{i=0}^2 L(x_i) + 5 \sum_{i=0}^2 L(v_i) \right. \\ &\quad \left. - 12 \sum_{i,j}^* L(y_{ij}) - 6 \sum_{i,j} L(z_{ij}) + 11 \right]. \end{aligned} \tag{8}$$

In order to understand the relation between this entropy and  $S_{3M}$  in (1) for the Kagomé lattice case, we may rewrite Eq. (8) as

$$\begin{aligned} S_M &= 2S_{3M} + kM \left[ \sum_i L(x_i) \right. \\ &\quad \left. + 5 \sum_i L(v_i) - 6 \sum_{i,j} L(z_{ij}) + 5 \right], \end{aligned} \tag{9}$$

in which the first term is for the two Kagomé layers as defined in Eq. (1) and the last  $kM[ \quad ]$  terms are the additional contribution due to the  $6M$  bonds connecting the two Kagomé layers to the middle layer.

The Hessian determinant to determine  $\rho_c$  is written as

$$\begin{vmatrix} \frac{4}{x_1} - \frac{4}{y_{01}} - \frac{1}{z_{10}} & \frac{4}{y_{01}} & 0 & \frac{1}{z_{01}} \\ \frac{4}{y_{01}} & -\frac{4}{y_{01}} - \frac{2}{y_{11}} & 0 & 0 \\ 0 & 0 & \frac{5}{6v_1} - \frac{1}{z_{01}} & \frac{1}{z_{01}} \\ \frac{1}{z_{10}} & 0 & \frac{1}{z_{01}} & -\frac{1}{z_{01}} - \frac{1}{z_{10}} - \frac{1}{z_{11}} \end{vmatrix} = 0, \tag{10}$$

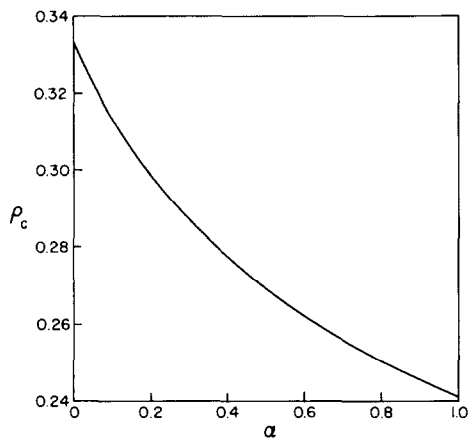


FIG. 2. Dependence of the percolation threshold  $\rho_c$  on  $\alpha$ .

where the elements are written at the non-percolating state. In evaluating this determinant for  $\rho_c$ , we use the expressions in Eqs. (4) and (7) keeping  $\xi_i = 0$  ( $i = 1, 2, 3$ , and 4). After an extensive algebraic transformation we can reduce Eq. (10) to an amazingly simple equation:

$$1 - 3\rho_c - 20\alpha\rho_c^3 = 0. \tag{11}$$

(I) We can first check that when  $\alpha = 0$ , namely when the middle layer is insulating, the  $\rho_c$  value reduces to the Kagomé layer value 1/3 of Eq. (5).

(II) When the middle layer points behave in the same way as the Kagomé lattice point,  $\alpha = 1$ , Eq. (11) gives the value

$$\rho_c(\alpha = 1) = 0.24055. \tag{12}$$

(III) The behavior of  $\rho_c$  as  $\alpha$  changes from 0 to 1 can be obtained by solving Eq. (11) as shown in Fig. 2.

(IV) The change of  $\rho_c$  from 1/3 for the Kagomé lattice ( $\alpha = 0$ ) to 0.24 for the three-layer structure ( $\alpha = 1$ ) is rather large. We want to understand why and in general how the middle layer points contribute to the formation of an extended cluster structure. For this purpose, we calculate the ratios of the

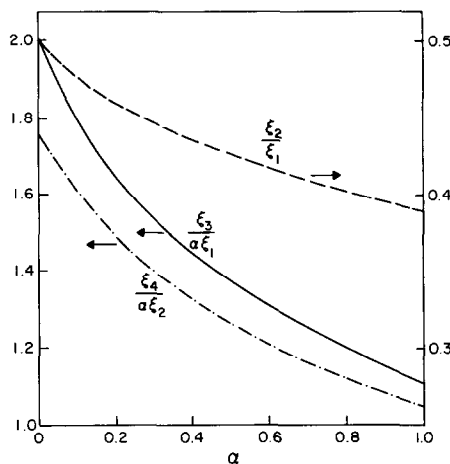


FIG. 3. Dependence of the ratios of the long range order variables,  $\xi_3/(\alpha\xi_1)$ ,  $\xi_4/(\alpha\xi_2)$ , and  $\xi_2/\xi_1$  given in Eq. (13), on  $\alpha$ .

long-range order variables,  $\xi_3/\xi_1$ ,  $\xi_4/\xi_2$ , and  $\xi_2/\xi_1$ , at  $\rho_c$ . These ratios are solved from the three equations containing the Hessian coefficients:

$$\begin{aligned} \left(\frac{4}{y_{01}} + \frac{2}{y_{11}}\right) \frac{\xi_2}{\xi_1} &= \frac{4}{y_{01}} \\ \left(\frac{5}{6v_1} - \frac{1}{z_{01}}\right) \frac{\xi_3}{\xi_1} + \frac{1}{z_{01}} \frac{\xi_4}{\xi_1} &= 0 \\ \frac{1}{z_{01}} \frac{\xi_3}{\xi_1} - \left(\frac{1}{z_{01}} + \frac{1}{z_{10}} + \frac{1}{z_{11}}\right) \frac{\xi_4}{\xi_1} &= -\frac{1}{z_{10}} \end{aligned} \tag{13}$$

At  $\rho_c$ , the ratios are solved as

$$\frac{\xi_3}{\alpha\xi_1} = \frac{24\rho^2}{1 + \rho} \tag{14a}$$

$$\frac{\xi_4}{\alpha\xi_2} = 2\rho(1 + 5\rho) \tag{14b}$$

$$\frac{\xi_2}{\xi_1} = \frac{2\rho}{1 + \rho}, \tag{14c}$$

The values of these ratios at  $\alpha = 0$  are 2, 16/9, and 1/2, respectively. Figure 3 shows how these values vary with  $\alpha$ .

We can interpret  $\xi_3/(\alpha\xi_1)$  and  $\xi_4/(\alpha\xi_2)$  as the measures of how strongly a middle layer point contributes to the percolation in comparison to a Kagomé layer point. The results that the values of these quantities are close to 2 near  $\alpha = 0$  mean that the middle layer points contribute to percolation twice as strongly as Kagomé lattice points. This is the reason why the  $\rho_c$  decreases rather steeply at  $\alpha = 0$  as  $\alpha$  increases ( $d\rho_c/d\alpha = 0.247$ ), and also why  $\rho_c$  decreases 28% as the middle layer participates in the percolation.

### Acknowledgments

The authors appreciate discussions with Dr. J. M. Honig with respect to the mechanism of electronic conduction in magnetite. They also thank Drs. T. Cole and R. M. Williams of Jet Propulsion Laboratory, California Institute of Technology, to bring the problem to the attention of the authors. M. Sankararaman is grateful for the support of the David Ross Grant of the Purdue Research Foundation. The theoretical work was supported by U.S. Department of Energy Grant DE-EG02-84ER45133.

### References

1. R. KIKUCHI, *Phys. Rev.* **81**, 988 (1951).
2. R. GALLI, P. LONGHI, T. MUSSINI, AND F. A. TROPEANO, *Electrochim. Acta* **18**, 1013 (1973).
3. J. H. KENNEDY AND S. M. STUBER, *J. Electrochem. Soc.* **128(11)**, 2303 (1981).
4. J. H. KENNEDY, J. R. AKRIDGE, AND M. KLIEZT, *Electrochim. Acta* **24**, 781 (1979).
5. J. H. KENNEDY, *J. Electrochem. Soc.* **124**, 865 (1979).
6. J. H. KENNEDY, N. KIMURA, AND S. M. STUBER, *J. Electrochem. Soc.* **129**, 1968 (1982).
7. J. H. KENNEDY AND S. M. STUBER, *Solid State Ionics* **5**, 171 (1981).
8. J. H. KENNEDY, S. M. STUBER, S. F. PASKER, AND P. H. BARETT, *Solid State Ionics* **8**, 323 (1983).
9. J. P. ROWLAND, Ph.D. Thesis, Purdue University, West Lafayette, IN (1977).
10. R. PASTOR, Ph.D. Thesis, Purdue University, West Lafayette, IN (1982).
11. J. P. ROWLAND, T. Y. TSENG, AND R. W. VEST, *J. Amer. Ceram. Soc.* **62**, 567 (1979).
12. C. A. BEEVERS AND M. A. S. ROSS, *Z. Kristallogr.* **97**, 59 (1937).
13. C. R. PETERS, M. BETTMAN, J. W. MOORE, AND M. D. GLICK, *Acta Crystallogr. Sect. B* **27**, 1826 (1971).
14. H. SATO AND R. KIKUCHI, *J. Chem. Phys.* **55**, 677 (1971).
15. H. SATO, *Solid State Ionics* **28-30**, 138 (1988).
16. R. ARAGON AND J. M. HONIG, *Phys. Rev. B* **37**, 209 (1988).
17. J. M. HONIG, *Phys. Chem. Miner.* **15**, 476 (1988).
18. D. R. WHITE, S. CHEN, H. R. HARRISON, AND H. SATO, *Solid State Ionics* **910**, 255 (1983).
19. S. CHEN, D. R. WHITE, H. SATO, J. B. LEWIS, AND W. R. ROBINSON, *J. Solid State Chem.* **62**, 26 (1986).
20. I. SHOZI, *Prog. Theor. Phys.* **6**, 306 (1951).
21. H. SATO, A. ARROTT, AND R. KIKUCHI, *J. Phys. Chem. Solids* **10**, 19 (1959).
22. H. SATO AND R. KIKUCHI, *Phys. Rev. B* **28**, 648 (1983).
23. R. KIKUCHI, *J. Chem. Phys.* **53**, 2713 (1970).
24. C. DOMB AND M. F. SYKES, *Phys. Rev.* **122**, 77 (1961).